

Displacement Energy Threshold for Ne⁺ Irradiation of Graphite

H. J. Steffen, D. Marton, and J. W. Rabalais

Department of Chemistry, University of Houston, Houston, Texas 77204-5641

(Received 21 June 1991)

A method for direct determination of the threshold energy (E_d) for displacing atoms by low-energy ion irradiation to form residual point defects is described. The method is demonstrated for Ne⁺ irradiation of graphite. The damage induced by low Ne⁺ doses ($< 2 \times 10^{15}$ ions/cm²) was quantified by means of a defect-sensitive feature in the Auger electron spectrum. The defect production rates at different Ne⁺ energies yield a displacement energy of $E_d = 35.3 \pm 1$ eV. This result provides new insight into the elementary collision processes leading to point defect creation.

PACS numbers: 61.80.Jh, 68.55.Ln, 79.20.Nc

Collision-induced atomic displacements are the major cause of crystal damage and property changes in materials following irradiation with energetic particles. The critical property for the particle energy- and flux-dependent defect production rate is the minimum energy necessary to irreversibly displace a lattice atom. This atomic displacement energy E_d is of fundamental importance in ion-beam-solid interactions because it affects various chemical and physical processes during sputtering, mixing, implantation, and film deposition [1,2]. For example, the number of defects created by an ion impinging on a solid will, according to the commonly used models (Kinchin and Pease [3] and others; see Refs. [4] and [5] for reviews), increase linearly with the energy transferred in the collision (T) for $T/E_d > n$, where $2 \leq n \leq 3$ is a model-dependent factor.

This Letter demonstrates, to the best of our knowledge, the first direct determination of threshold displacement energies E_d using low-energy ions. Previous measurements of E_d have been carried out using high-energy electrons as projectiles [4]; it was assumed that E_d does not depend on the nature (mass, chemical properties) of the projectile, and, therefore, E_d values obtained in these experiments could be used to interpret ion-induced damage. Although this assumption is over 40 years old, it has never been tested until now. Since the projectile-surface encounter can include attractive and repulsive forces, long-range multiple-atom interactions, and chemical reactions, it is highly likely that E_d depends on the nature of the projectile.

The E_d has great significance in developing theoretical models for elucidating ion-beam effects which constitute the basis for a range of contemporary technologies. Although E_d is an input parameter in many classical ion trajectory simulations used in modeling ion-surface interactions, there is a very limited theoretical understanding [4,5]. This is partially due to the complex interaction potentials required for low-energy ion-surface collisions. Experimental E_d values for various projectile-target pairs will help to alleviate this problem.

The unique feature of our method for E_d measurement is the controlled damage by well-defined small doses of

monoenergetic ions. By using kinetic energies close to the threshold energy of defect formation, the damage is limited to the surface region and the number of displacements is reduced to mainly primary knockon events. This preserves a low concentration of defects, ensuring negligible defect-defect interactions. The use of noble-gas Ne⁺ ions limits the possibility of chemical interactions with lattice atoms. The ion-induced damage is monitored with Auger electron spectroscopy (AES) in which high surface sensitivity is characterized by the electron attenuation length [6] of ~ 5.5 Å and the detection limit of $\sim 10^{12}$ atoms/cm².

The experiments were performed using a magnetically mass- and energy-selected ion beam [7] at a base pressure of $\sim 2 \times 10^{-9}$ Torr. For each experiment at a selected primary ion energy, a highly oriented pyrolytic graphite sample with a rectangular area of ca. 1.2 mm² was cleaved along the basal plane, mounted on the specimen stage, and the native surface was then irradiated with Ne⁺ at normal incidence. The ion doses were measured by time integration of the current on the sample. The electron-excited AES spectrum of the carbon *KVV* Auger transition was recorded in the pulse-counting mode with a cylindrical mirror analyzer at 0.6% energy resolution, smoothed, and differentiated. The primary electron energy for AES was 3 keV and the current density was ca. 1.3 mA/cm². The experimental details have been described elsewhere [7].

As we have recently shown [7], a peak in the C *KVV* spectrum at ca. 279 eV kinetic energy and ca. 3.8 eV below the Auger threshold emerges after ion irradiation of graphite. This feature is related to point defects; atoms occupying defect sites have nonbonding orbitals which result in electronic defect states near the Fermi energy. The intensity of this feature provides a measure of the ion-induced damage which can be quantified by using a shape factor s with $s = I_1/I_0$, where I_1 and I_0 are defined as shown in Fig. 1. Changes in the number of defects caused by ion irradiation are then described by the shape factor ratio $S = (s - s_G)/s_G$, where s_G is the shape factor for the undamaged graphite spectrum. The evolution of S in the course of the ion bombardment is shown

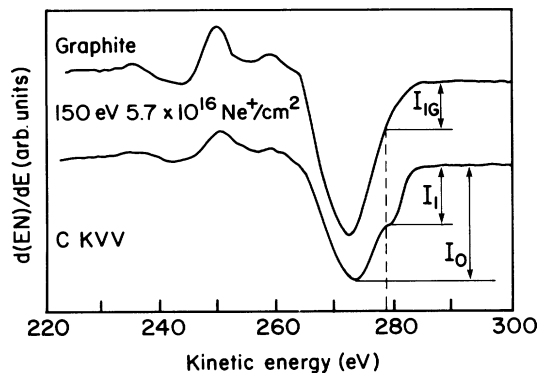


FIG. 1. AES KLL carbon lines illustrating the definition of the shape factor s . The shape factor ratio S is determined as $(s - s_G)/s_G$, where s_G is the shape factor for the original graphite sample.

in Fig. 2 for five primary ion energies between 40 and 150 eV. The experiment with 30 eV Ne^+ did not lead to a measurable Auger line-shape change. As apparent from Fig. 2, the irradiation for each ion energy results in a near-linear increase in S at low doses. For higher doses, when $S \geq 0.3$, the respective curves saturate [7] (not shown in Fig. 2). The straight lines are least-squares fits to the experimental points in this initial stage including $S=0$ for the initial state. The number of freshly created lattice defects should be proportional to the flux of impinging ions. Only an initial linear change is expected for such a material property which is sensitive to structural disorder. In this case, the linearity confirms the validity of our method in assessing the relative defect concentration and the assumption of noninteracting point defects in the initial stage. At higher ion doses and, therefore, at

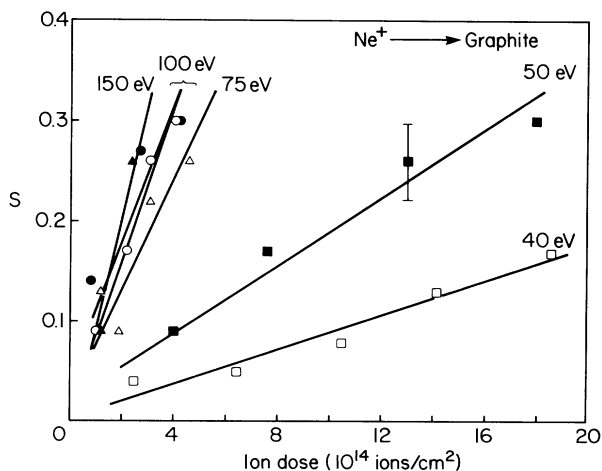


FIG. 2. The AES shape factor ratio S or defect concentration versus Ne^+ ion dose at different ion energies (\square , 40 eV; \blacksquare , 50 eV; Δ , 75 eV; \bullet and \circ , 100 eV; and \blacktriangle , 150 eV). Note that only $(s - s_G)/s_G \leq 0.3$ is shown in order to stay within the linear region. The error bar applies to all data shown.

higher defect concentrations, point defect annihilation and cluster formation may be more prevalent and may lead to the observed deviation from linear behavior. The slope for each curve in Fig. 2 characterizes the susceptibility for defect creation and can be defined as a relative measure of the defect production rate.

The defect production rate depends on the primary ion energy. This is illustrated in Fig. 3 where the defect production rates, i.e., the slopes of the lines of Fig. 2 normalized to the slope at 150 eV, are plotted against the primary Ne^+ ion energy. A distinct threshold energy for the defect production rate is obtained, below which lattice disorder cannot be detected by our AES measurements. Above this threshold energy, at about 40 eV, the defect production rate increases sharply. The error bars in Fig. 2 are primarily determined by the AES measurement noise. The sizes of the error bars in Fig. 3 increase with increasing energy because the applied ion doses decrease. The precision of the technique can be improved if AES spectra are acquired with higher energy resolution and signal-to-noise ratios.

Within our experimental error, several descriptions of the near-threshold region are possible. This ambiguity is related to the fact that there is no rigorous theory available which can be applied to the data. Such a theory should not only consider defect production by calculation of the energy- and angle-dependent displacement cross section [8], but must also include annealing effects. Using a simplified approach, the defect production rate (R) can be related to the probability (P) for creation of a defect in a collision with energy transfer (T) and to the collision cross section (σ) in the following manner [9]:

$$R \sim \int_{E_d}^T P(T) \frac{d\sigma}{dT} dT. \tag{1}$$

This expression involves the assumptions that (1) per-

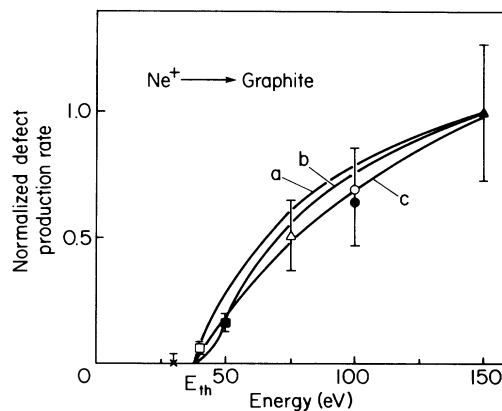


FIG. 3. Defect production rate as a function of Ne^+ energy. The data points (except for 30 eV) are the slopes of the least-squares lines of Fig. 1 normalized to the value at 150 eV. The lines are calculated with the following: curve a, $m=0.2$, $E_{th}=38$ eV, $\Delta=0$; curve b, $m=0.2$, $E_{th}=38$ eV, $\Delta=5$ eV; curve c, $m=0$, $E_{th}=38.2$ eV, $\Delta=0$.

manent defects (i.e., those actually detected minutes after the damage was inflicted) are created with rates proportional to the overall defect production rates and (2) the efficiency of defect detection is constant over the energy range analyzed. Assumption (1) is supported by the observed linearity of damage dependence on ion flux (Fig. 2) and assumption (2) by comparison of projected ion ranges (a maximum of 8 Å at 150 eV) with Auger electron attenuation length (~ 5.5 Å).

Equation (1) can be evaluated in relative terms using simplified assumptions for $P(T)$ and $\sigma(T)$. For $P(T)$ it is usual to assume [4] either (a)

$$\begin{aligned} P &= 0 \text{ for } T < E_d, \\ P &= 1 \text{ for } T \geq E_d \end{aligned} \quad (2)$$

or (b)

$$\begin{aligned} P &= 0 \text{ for } T < E_d, \\ P &= (T - E_d)/2\Delta \text{ for } E_d \leq T < E_d + 2\Delta, \\ P &= 1 \text{ for } T \geq E_d + 2\Delta, \end{aligned} \quad (3)$$

where 2Δ (a fitting parameter) is the linear region for P . For $\sigma(T)$, very little reliable information exists for $E < 150$ eV. We employ the Lindhard approach [10], where the potential is described by a power function of the separation of the interacting atoms, r . This leads to an analytical solution for the cross section in the form of

$$d\sigma(T) \sim E^{-m} T^{-1-m} dT, \quad (4)$$

where $0 \leq m \leq 1$ is the scaling parameter of the screening length (a) in the potential. The value of m was optimized for the Ne-C pair by fitting by the Biersack-Ziegler universal potential [11]. Using $m=0.2$, the Lindhard potential provides a good approximation to the Biersack-Ziegler potential over the wide range of $10 < r/a < 40$. Curves *a* and *b* of Fig. 3 were obtained from the corresponding probability functions of Eqs. (2) and (3), respectively. Using $m=0$ provides the best match to the universal potential at higher r/a values, i.e., lower impact energies. Curve *c* of Fig. 3 was obtained with $P(T)$ according to Eq. (2) and $m=0$, yielding a simple logarithmic relationship. Although the precision of the data does not allow us to exclude other cases, curve *c* provides the best approximation to the data. The value of $E_{th} = 37.7 \pm 1$ eV yields, considering the kinematic factor $4M_1M_2/(M_1+M_2)^2$, a corresponding E_d value of $E_d = 35.3 \pm 1$ eV. This value would not change significantly if other fits were employed.

A comparison of our E_d value with the electron-induced literature values for graphite [12,13], which range from 24.7 to 33 eV, should be based on the analysis of differences in the physical processes due to low-energy ion impact versus high-energy electron impact and the specific nature of graphite. Low-energy ions create surface defects, while high-energy electrons create bulk de-

fects. However, evidence suggests that E_d due to electrons at the graphite surface is the same as E_d in the bulk [14]. The nature of the projectile mainly affects the primary collision event. The movement of the recoil atom into a stable defect position does not depend on the nature of the projectile. We suggest that E_d can be partitioned into three components as

$$E_d = E_F + (E_e^i + E_e^f) + (E_r^i + E_r^f), \quad (5)$$

where E_F is the adiabatic work required for formation of a Frenkel pair, which includes the site-dependent atomic binding energy, and the latter two terms represent the inelastic energy losses due to electron and phonon excitation during the primary collision ($E_e^i + E_e^f$) and as the recoiled atom moves to a stable interstitial site ($E_r^i + E_r^f$). The location of such a site can be temperature dependent due to recombination processes. E_d therefore depends on temperature and recoiling direction in the crystal lattice.

Consider the primary collision event. Whereas electrons lose energy inelastically by direct electron excitation and ionization, there are several different inelastic channels available to ions. First, ions form transient quasi-molecules with the target atoms resulting in electron promotion to highly excited states [15]. Second, direct long-range interactions between the ion and neighboring lattice atoms can excite phonons. Third, at very low energies the attractive component of the interatomic potential becomes significant; recent molecular-dynamics simulations [16] have shown that such bonding interactions provide additional inelastic energy-loss channels in collision cascades. These additional inelastic energy-loss mechanisms can account for several eV and are most likely responsible for the slightly higher E_d determined by ion impact compared to electron impact.

Consider the recoil event. The activation energy for interstitial migration along the basal planes of graphite [17] is < 0.1 eV. Consequently, only a small fraction of the initial displacements within a basal plane remain due to simultaneous annealing processes. In contrast, migration of vacancies and interstitials parallel to the crystal c axis is excluded at room temperature because of the high activation energies required [17], i.e., $E_r > 5.5$ eV and $E_i > 5$ eV, where E_r and E_i correspond to vacancies and interstitials, respectively. Therefore, stable Frenkel pairs can exist at room temperature only when the vacancy and interstitial are separated by at least one basal plane, this process requiring > 5 eV. Electronic losses by the recoil are estimated [18] to be of the order of 10% for low- Z materials and low energies. Therefore, energy losses by the recoil in forming a stable Frenkel defect are of the order of several eV.

The energy required for Frenkel-pair formation in graphite [17] is $E_F = 14$ eV. It is generally found [5] that $E_d/E_F \sim 2-4$, in accord with our measurement. The E_F of graphite is exceptionally high and is responsible for the high E_d compared to other covalently bonded solids with

similar atomic densities [4] ($E_d \sim 14$ eV) and close-packed metals [19] ($E_d \geq 20$ eV). The layered structure of graphite and the high mobility of interstitials may account for this.

In order to minimize annihilation and determine the absolute minimum E_d , experiments must be performed near 0 K. However, E_d values determined at higher temperatures may be more useful for practical applications, e.g., in film deposition where partial annealing occurs. With an optimal choice of the primary ion energy during ion-beam deposition or ion-assisted MBE, epitaxial ordering may be facilitated due to enhanced surface displacements, whereas defect formation in the subsurface region is avoided or minimized [20].

To the best of our knowledge, this is the first use of low-energy ions at low doses to determine the displacement energy E_d . The method described herein is general and can be applied to any material for which a sensitive measure of the surface defect concentration can be obtained. Indeed, the electron spectra of some semiconductors and insulators are known [21,22] to exhibit defect-sensitive features. Further studies with semiconductor substrates, e.g., Si, Ge, GaAs, and other types of ions will be performed in order to elucidate the nature of the interactions affecting E_d .

This material is based on work supported by the National Science Foundation under Grant No. DMR-8914608.

[1] *Ion Bombardment Modification of Surfaces: Fundamentals and Applications*, edited by O. Auciello and R. Kelly (Elsevier, Amsterdam, 1984).

[2] *Ion Beam Assisted Film Growth*, edited by T. Itoh (Elsevier, Amsterdam, 1989).

[3] G. H. Kinchin and R. S. Pease, *Rep. Prog. Phys.* **18**, 1 (1955).

[4] J. W. Corbett and J. C. Bourgoin, in *Point Defects in Solids*, edited by J. H. Crawford, Jr. and L. M. Slifkin (Plenum, New York, 1975), Vol. 2, Chap. 1.

[5] V. L. Vinetskii and G. A. Kholodar, in *Physics of Radiation Effects in Crystals*, edited by R. A. Johnson and A. N. Orlov (North-Holland, Amsterdam, 1986), p. 285.

[6] S. Tanuma, C. J. Powell, and D. R. Penn, *Surf. Interface Anal.* **11**, 577 (1988).

[7] H. J. Steffen, C. D. Roux, D. Marton, and J. W. Rabalais, *Phys. Rev. B* **44**, 3981 (1991).

[8] T. Iwata and T. Nihira, *J. Phys. Soc. Jpn.* **31**, 1761 (1971).

[9] W. E. Faust, T. N. O'Neal, and R. L. Chaplin, *Phys. Rev.* **183**, 609 (1969).

[10] H. Winters, in *Radiation Effects on Solid Surfaces*, edited by M. Kaminsky, *Advances in Chemistry Series Vol. 158* (ACS, Washington, DC, 1976), p.1.

[11] D. J. O'Connor and J. P. Biersack, *Nucl. Instrum. Methods Phys. Res., Sect. B* **15**, 14 (1986).

[12] J. H. W. Simmons, *Radiation Damage in Graphite* (Pergamon, Oxford, 1965).

[13] B. T. Kelly, *Physics of Graphite* (Applied Science Publications, London, 1981).

[14] G. L. Montel and G. E. Myers, *Carbon* **9**, 179 (1971).

[15] R. Souda, T. Aizawa, C. Oshima, and Y. Ishizawa, *Nucl. Instrum. Methods Phys. Res., Sect. B* **45**, 364 (1990).

[16] B. W. Dodson, *Crit. Rev. Solid State Mat. Sci.* **16**, 115 (1990).

[17] P. A. Thrower and R. M. Mayer, *Phys. Status Solidi* **47**, 11 (1978).

[18] H. H. Andersen, *Nucl. Instrum. Methods Phys. Res., Sect. B* **18**, 321 (1987).

[19] H. H. Andersen, *Appl. Phys.* **18**, 131 (1979).

[20] N. Herbots, O. C. Hellman, P. A. Cullen, and O. Vancauwenbergh, in *Deposition and Growth: Limits for Microelectronics*, edited by G. W. Rubloff (AIP, New York, 1988), p. 259.

[21] V. M. Bermudez, *Prog. Surf. Sci.* **11**, 7 (1987).

[22] V. E. Henrich, *Rep. Prog. Phys.* **48**, 1487 (1985).